

State Key Laboratory of Genetic Engineering¹; Department of Biochemistry², School of Life Sciences, Fudan University, Shanghai, P. R. China

Preparation and characterization of paclitaxel delivery system based on semi-solid lipid nanoparticles coated with poly (ethylene glycol)

LIFANG WU^{1,2}, CUI TANG¹, CHUNHUA YIN^{1,2}

Received October 24, 2009, accepted October 27, 2009

Lifang Wu, Chunhua Yin, State Key Laboratory of Genetic Engineering, Department of Biochemistry, School of Life Sciences, Fudan University, Shanghai, P. R. China
wlfang2008@sina.com, chyin@fudan.edu.cn

Pharmazie 65: 493–499 (2010)

doi: 10.1691/ph.2010.9341

The current formulation of paclitaxel causes significant side effects, so there is a need to develop a safer delivery system. In this study, novel semi-solid lipid nanoparticles (PEG-PE-SSLN) were prepared, and evaluated as delivery vehicles for paclitaxel. The PEG-PE-SSLN are approximately 213 nm in size with a zeta-potential of -37 mV, compared to Span60-SSLN with a particle size of over 275 nm and zeta-potential of -29 mV. The encapsulation efficiency of PEG-PE-SSLN could be as high as 98%. Furthermore, differential scanning calorimetry (DSC) analysis indicated that paclitaxel in the nanoparticles existed in an amorphous form. A sustained release of 85% of the loaded paclitaxel from PEG-PE-SSLN within 12 days was observed while release from Span60-SSLN particles was complete within 6 days. PEG-PE-SSLN can effectively decrease phagocytosis of murine peritoneal macrophages. Lyophilization of SSLNs in the presence of trehalose tended to preserve their stability. Therefore, PEG-PE-SSLN represents an improved and promising paclitaxel delivery system.

1. Introduction

Paclitaxel (PTX), a commonly used anticancer drug, exhibits widespread and significant anti-neoplastic activities, particularly against primary epithelial ovarian carcinoma, breast, colon, head, and non-small cell lung cancer, and AIDS related Kaposi's sarcoma (Spencer and Faulds 1994). Due to its low aqueous solubility, PTX is currently formulated in a 1:1 mixture of Cremophor EL[®] (polyethoxylated castor oil) and ethanol as a commercially available product named Taxol[®], which is diluted 2–20 fold in saline or dextrose solution (5%) before administration (Szebeni et al. 1998). However, this formulation shows limited stability when diluted and significant toxicity is caused by the vehicle (Song et al. 1996). More recently, the FDA approved a product with a new formulation, named ABI-007 (Abraxane[®], Abraxis Bioscience Inc., Los Angeles, USA), for breast cancer treatment. Compared to Taxol[®], Abraxane[®], an albumin-bound particle form of PTX, displays greater efficacy and a more favorable safety profile (Gradishar et al. 2005; Gradishar 2006). Because of the high cost and limited availability of human albumin used for the particles, development of a better techno-economical formulation for PTX delivery is deemed necessary and meaningful.

Solid lipid nanoparticles (SLNs) are increasingly popular as novel carriers for hydrophobic drugs due to various advantages such as convenience of administration, low cost of large scale production and low toxicity as well as long half-life in blood circulation (Müller et al. 2000; Lamprecht et al. 2002). Therefore, SLNs for delivery of anticancer drugs have attracted intense interest and have become an important area in cancer nanotechnology (Zhang and Feng 2006).

However, the drug loading capacities of conventional SLNs are limited for the highly ordered crystal lattice of lipid layers,

ranging from 25% to 50% (Mehnert et al. 1997; Westesen et al. 1997). Also, the limited stability of SLNs during storage and administration restricts their application both *in vitro* and *in vivo* (Klivanov et al. 1991). Therefore, use of complex lipids is expected to improve drug loading. For example, incorporating triglyceride-containing oils in the solid core of the complex lipids can effectively increase payloads (Jenning et al. 2000; Garcia-Fuentes et al. 2005). Among the various attempts to enhance particle stability, coating with poly (ethylene glycol) (PEG) has proved successful. With their conformational flexibility and water-binding ability, PEG chains are believed to prevent or diminish the adsorption of opsonizing proteins which direct the particles to macrophages (Allen 1994). PEG-coated nanoparticles exhibit dose-independent prolonged half-life in blood circulations, reduced uptake by macrophages in the liver and spleen, and increased accumulation in tumors (Klivanov et al. 1991; Woodle and Lasic 1992; Gabizon et al. 1994).

In this study, novel semi-solid lipid nanoparticles (SSLNs) modified with PEG were prepared as delivery carriers for PTX. Particle size, zeta potential, PTX encapsulation efficiency and *in vitro* release behavior of the PEG-coated SSLNs were investigated. Differential scanning calorimetry (DSC) was used to detect possible changes in the crystallization of the solid lipid and molecular interactions between different lipids. The effect of PEG coating on phagocytosis of the particles was also studied *in vitro* using the mouse peritoneal macrophage system.

2. Investigations, results and discussion

2.1. Preparation of semi-solid lipid nanoparticles

The particle size, size distribution, encapsulation efficiency (EE), and morphology of PTX nanoparticles were optimized

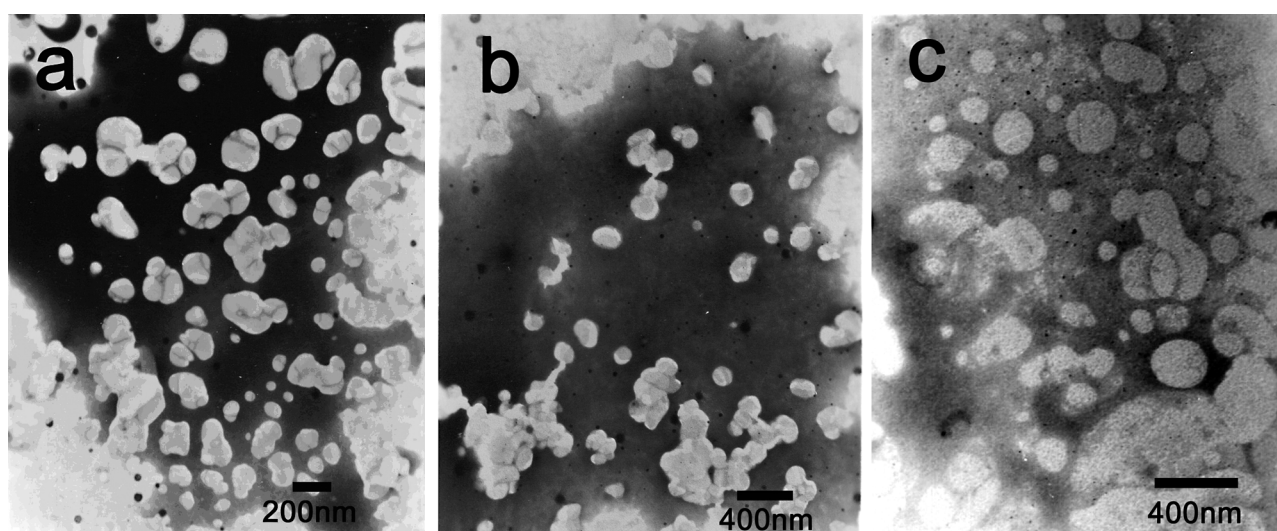


Fig. 1: TEM images of (a) Blank-SSLN, (b) PEG-PE-SSLN, and (c) Span60-SSLN

Table 1: Factors and levels Table of L9 (3⁴) orthogonal design for optimizing the formulation of PTX-SSLN

| Level | A | B | C | D |
|-------|-----------------|----------|------------------|-------------|
| | Dynasan118 (mg) | PTX (mg) | Miglyol812N (μl) | PEG-PE (mg) |
| 1 | 50 | 10 | 100 | 100 |
| 2 | 100 | 15 | 200 | 200 |
| 3 | 200 | 20 | 400 | 300 |

by varying the experimental conditions. Through single-factor experiments, we found that the amount of Dynasan118, PTX, Miglyol812N and emulsifier had a big effect on EE (Table 1). It has been reported that the co-emulsifier soybean lecithin displayed an “on-off” effect on the formation of nanoparticles (Chen et al. 2002), and this was also confirmed by our results. In this study the amount of soybean lecithin co-emulsifier was chosen as 100 mg in all the formulations. Taking the results of single-factor experiments and orthogonal experiments together, the optimal formulation was confirmed to be

A₃B₁C₂D₂ according to Table 2 using PTX EE as the assessment criterion. The formulation was Dynasan118, 200 mg; PTX, 10 mg; Miglyol812N, 100 μl; emulsifier, 200 mg. In the following studies, this formulation was used throughout. Liquid and solid lipids were combined to form a homogenous solid carrier with liquid nanocompartments, which enhanced the encapsulation efficiency. Miglyol812N was chosen as the liquid lipid for its good solubility and chemical structure. A fine dispersion could be obtained when increasing the reaction temperature and stirring rate during nanoparticle formation. A temperature of 70 °C and stirring rate of 1,000 rpm were required during emulsification.

2.2. Physicochemical characteristics of semi-solid lipid nanoparticles

TEM was used to visualize the nanoparticles. Fig. 1 clearly illustrate that the morphology of Span60-SSLN is polygonal (Fig. 1c), while both blank-SSLN and PEG-PE-SSLN (Fig. 1a and b, respectively) appeared round and homogeneous. As shown by the arrows in Fig. 2, the PEG “shells” on the surface of the nanoparticles were also observed. In order to obtain more

Table 2: Results of L9 (3⁴) orthogonal design

| No. | Actual Variable | | | | Result | | | |
|--------|-----------------|--------|--------|--------|---------------------|---------------------|---------------------|--------|
| | A | B | C | D | EE ₁ (%) | EE ₂ (%) | EE ₃ (%) | Y |
| 1 | 1 | 1 | 1 | 1 | 87.03 | 91.48 | 85.04 | 263.55 |
| 2 | 1 | 2 | 2 | 2 | 95.49 | 94.71 | 94.26 | 284.46 |
| 3 | 1 | 3 | 3 | 3 | 83.09 | 83.57 | 86.63 | 263.29 |
| 4 | 2 | 1 | 2 | 3 | 93.75 | 86.69 | 95.74 | 276.18 |
| 5 | 2 | 2 | 3 | 1 | 75.69 | 78.83 | 74.12 | 228.64 |
| 6 | 2 | 3 | 1 | 2 | 91.97 | 96.73 | 93.60 | 282.3 |
| 7 | 3 | 1 | 3 | 2 | 92.10 | 95.25 | 91.76 | 279.11 |
| 8 | 3 | 2 | 1 | 3 | 97.10 | 97.30 | 97.09 | 291.49 |
| 9 | 3 | 3 | 2 | 1 | 98.08 | 86.23 | 92.76 | 277.07 |
| I | 811.30 | 818.84 | 837.34 | 769.26 | | | | |
| II | 787.12 | 804.59 | 837.71 | 845.87 | | | | |
| III | 847.67 | 822.66 | 771.04 | 830.96 | | | | |
| I av | 270.43 | 272.95 | 279.11 | 256.42 | | | | |
| II av | 262.37 | 268.20 | 279.24 | 281.96 | | | | |
| III av | 282.56 | 274.22 | 257.01 | 276.99 | | | | |
| R | 20.19 | 6.02 | 22.23 | 25.54 | | | | |

A: Dynasan118; B: PTX; C: Miglyol812N; D: PEG-PE; EE: Encapsulation efficiency; Y = EE₁ + EE₂ + EE₃

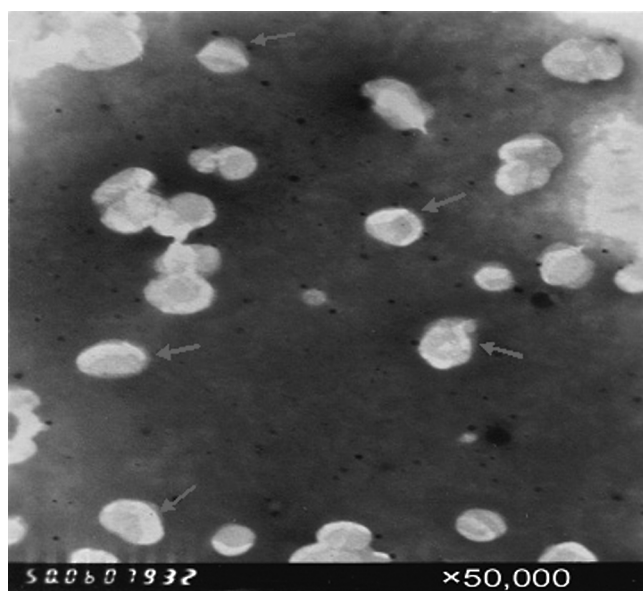


Fig. 2: TEM image of PEG-PE-SSLN ($\times 50,000$)

precise information on the size distribution, further analysis was performed.

Table 3 and Fig. 3 show that the mean particle size of blank-SSLN was about 190 nm. After drug loading, the mean particle size became slightly larger, approximately 275 nm and 210 nm for Span60-SSLN and PEG-PE-SSLN, respectively. Fig. 3 demonstrates that PEG-PE-SSLN (Fig. 3b) showed a smaller particle size than Span60-SSLN (Fig. 3c), though Span60-SSLN had a narrower size distribution than PEG-PE-SSLN.

As illustrated in Table 3, zeta potentials of all samples were negative. Since PEG was uncharged, the negative charge may be attributed to the presence of ionized carboxyl groups, such as those from stearic acid or caprylic acid, on the nanoparticle surface. The zeta potential of blank-SSLN was about -28 mV, while those of drug-loaded PEG-PE-SSLN and Span60-SSLN were -37 mV and -29 mV, respectively. It has been reported that PEG coating the surface of the nanoparticles can result in a decrease of zeta potential (Ana et al. 2004), though in this study the zeta potential of PEG-PE-SSLN was larger than that of Span60-SSLN without PEG chains. Such a result could be explained by the fact that the positive charges of the $-NH_2$ group is greatly reduced when PEG binds the $-NH_2$ group of phosphatidylethanolamine.

Table 3 also shows that the drug EE of PEG-PE-SSLN was as high as 98% and that of Span60-SSLN was more than 95%. As a less ordered structure of the nanoparticles facilitates drug loading (Westesen et al. 1997), addition of Miglyol812N decreased the ordered structure of the lipid matrix and thus increased the drug encapsulation efficiency in the present study.

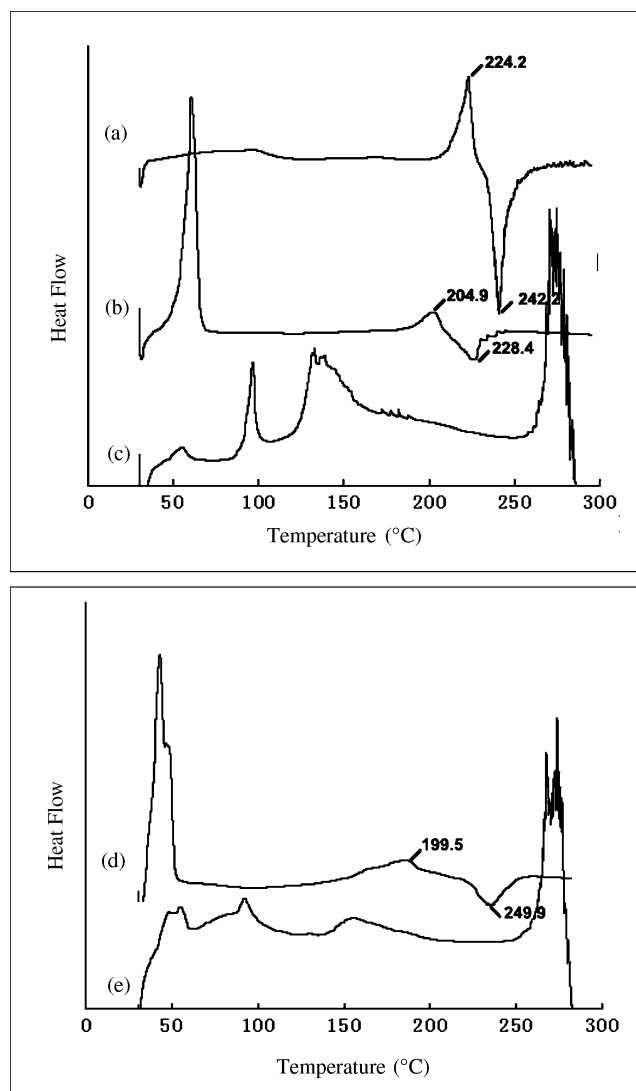


Fig. 4: DSC thermograms of (a) PTX, (b) Physical mixture of Span60, Dynasan118 and PTX, (c) Lyophilizate of Span60-SSLN, (d) Physical mixture of PEG-PE, Dynasan118 and PTX, and (e) Lyophilizate of PEG-PE-SSLN

DSC is often used to investigate the melting and recrystallization behavior of crystalline materials like lipid nanoparticles (Dubernet 1995). As shown in Fig. 4a, the characteristic peaks of PTX crystals appeared at 224°C and 242°C , consistent with previous reports (Liggins et al. 1997). The physical mixtures of Dynasan118, PTX and the emulsifiers Span60 and PEG-PE, respectively, also presented the characteristic peaks of PTX (Fig. 4b, d) with slight shifts, which might be attributed to interactions among the various components. However, the characteristic peak of PTX disappeared after being encapsulated in

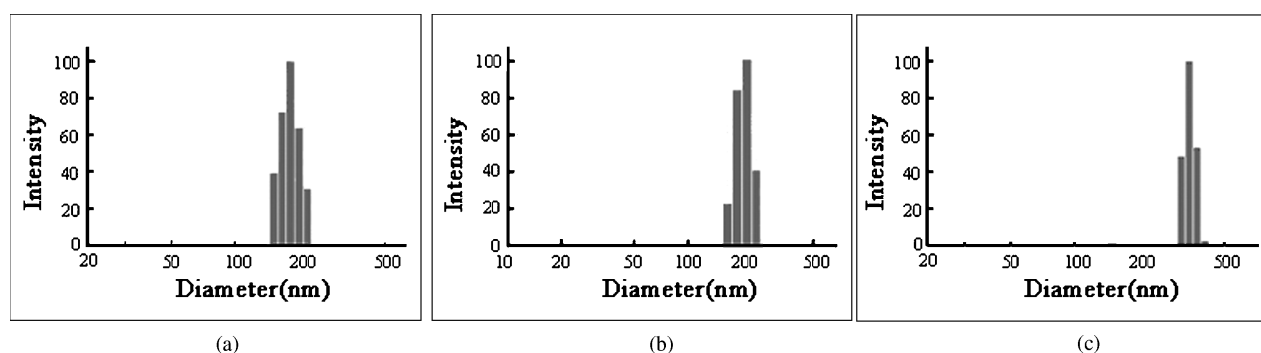


Fig. 3: Laser diversity charts for measuring diameter and distribution of (a) Blank-SSLN, (b) PEG-PE-SSLN, and (c) Span60-SSLN

Table 3: Transformation of encapsulation efficiency, particle size and zeta potential for different SSLNs before and after lyophilization using trehalose as cryoprotector

| SSLN | EE (%) | | Particle size (nm) | | Zeta potential (mV) | |
|--------|------------|------------|--------------------|--------------|---------------------|-------------|
| | Before | After | Before | After | Before | After |
| Blank | — | — | 189.9 ± 29.5 | 226.2 ± 21.5 | −28.4 ± 2.3 | −25.1 ± 1.0 |
| PEG-PE | 98.1 ± 0.1 | 96.2 ± 0.3 | 213.3 ± 18.3 | 225.0 ± 14.0 | −37.5 ± 2.6 | −32.4 ± 0.5 |
| Span60 | 95.5 ± 0.2 | 86.1 ± 1.4 | 275.5 ± 3.1 | 327.4 ± 2.8 | −29.2 ± 0.2 | −27.2 ± 4.0 |

Data represented mean size ± SD (n = 3)
EE: encapsulation efficiency

the lipid nanoparticles as Fig. 4c and e showed, indicating that the drug existed in the amorphous rather than crystal form in both nanoparticles.

Only 4.7% of the encapsulated PTX was released within 6 days in pH 7.4 phosphate buffered saline (PBS), which was attributed particularly to the low solubility of the drug in the aqueous phase (Lamprecht et al. 2002). Therefore, 0.1% (w/v) Tween80 was added to the release medium to increase its solubility and to avoid binding of PTX to the membrane (Sahoo et al. 2004). Fig. 5 shows the *in vitro* release of PTX from Span60-SSLN and PEG-PE-SSLN, respectively. A fast initial release of the drug was observed in the first 2 days while sustained release at a slower release rate was found thereafter. The initial release was probably due to drug molecules in the nanoparticle shell while the sustained release profile thereafter may be attributed to diffusion of PTX molecules entrapped in the oily core. Also, PTX was completely released from Span60-SSLN within 6 days while only 85% of the drug was released from PEG-PE-SSLN within 12 days. This result may be interpreted as PEG chains effectively prolonging the *in vitro* release time of PTX from the nanoparticles, in accordance with literature reports (Allen 1994).

2.3. Phagocytosis of semi-solid lipid nanoparticles

Nanoparticles delivered by intravenous injection are taken up by the liver, spleen, and other parts of the reticulo-endothelial system depending on particle sizes and surface properties (Rudt and Müller 1992; Evora et al. 1998). To reduce the clearance of nanoparticles by macrophages, the drug carrier is coated with hydrophilic polymers such as PEG. Increasing polymer

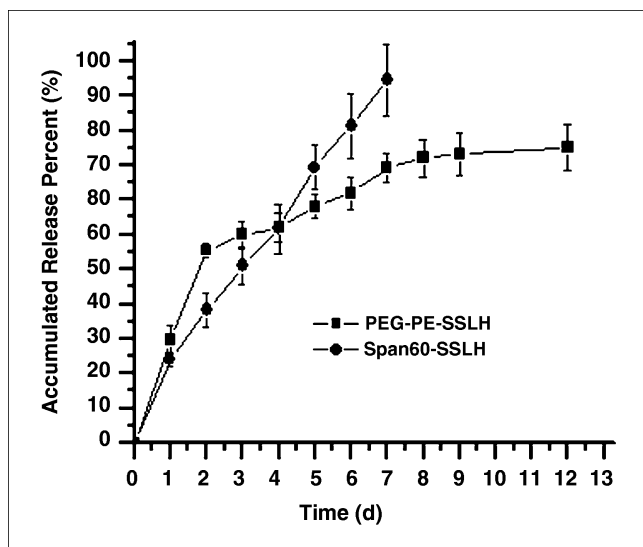


Fig. 5: *In vitro* release profiles of PTX-loaded PEG-PE-SSLN (■) and Span60-SSLN (●) in pH 7.4 PBS containing 0.1% Tween80. Values mean ± S.D., n = 3

hydrophilicity would lower the number of cells involved in detectable particle uptake of nanoparticles (Prior et al. 2002), which is consistent with reduced phagocytic clearance from the bloodstream of hydrophobic particles coated with hydrophilic PEG or related polymers (Illum et al. 1987). Fig. 6 shows the uptake of the SSLNs with different emulsifiers by mouse peritoneal macrophages. The uptake rates of Span60-SSLN and PEG-PE-SSLN without plasma were 2.31% and 0.65% within 30 min, respectively, indicating that PEG-PE-SSLN inhibited phagocytosis to a greater extent than Span60-SSLN, in accordance with previous research (Bocca et al. 1998). When plasma was added, the uptake levels of Span60-SSLN and PEG-PE-SSLN were 3.21% and 1.61% in 30 min, respectively, which was a similar trend to the above results in the absence of plasma. Therefore, it was concluded that incubation of lipid nanoparticles with monocyte-macrophages led to particle uptake and cell activation. However, the steric hindrance of PEG could effectively reduce plasma protein absorption so as to decrease phagocytosis of the mononuclear phagocyte system. PEG-PE-SSLN is expected to prolong the circulation time in blood and to potentially enhance tumor targeting efficiency due to its reduced phagocytosis (Zara et al. 2002).

2.4. Lyophilization of semi-solid lipid nanoparticles

Lyophilized powder is more stable than nanoparticle suspensions, so we tried to freeze-dry the nanoparticle suspension following screening of suitable cryoprotectants. Saccharides have been applied extensively as cryoprotectants to reduce particle aggregation of lipid nanoparticles (Schwarz and Mehnert 1997) because lyophilization may destroy the outer surfactant film resulting in increase in particle size (Freitas and Müller 1998). Different cryoprotectants including sorbitol, mannitol,

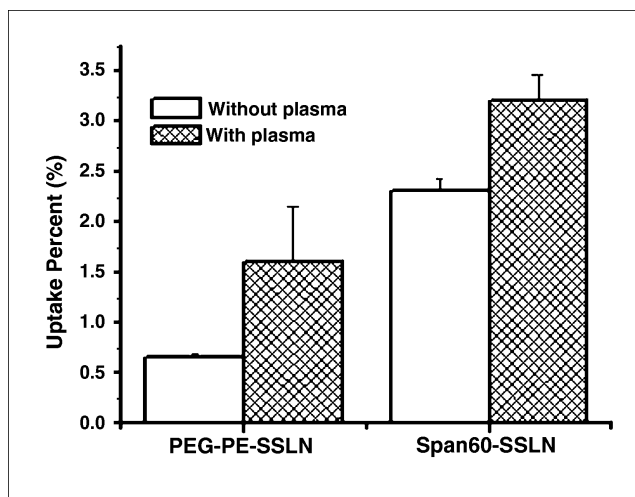


Fig. 6: Uptake of PEG-PE-SSLN and Span60-SSLN by mouse peritoneal macrophages with and without plasma. Values mean ± S.D., n = 3

Table 4: Final to initial size ratios of PEG-PE-SSLN after lyophilization with different cryoprotectors and at various concentrations

| Cryoprotectors | Concentration | Final to initial size ratios |
|------------------|---------------|------------------------------|
| Dextran | 2% | ND |
| | 5% | ND |
| | 10% | 15.81 |
| Glucose | 2% | 2.27 |
| | 5% | 1.56 |
| | 10% | 1.41 |
| Trehalose | 2% | 2.21 |
| | 5% | 1.22 |
| | 10% | 1.06 |
| Mannitol | 2% | 2.34 |
| | 5% | 1.94 |
| | 10% | 2.99 |
| Sucrose | 2% | 1.73 |
| | 5% | 1.92 |
| | 10% | 1.58 |
| Sorbitol | 2% | 1.81 |
| | 5% | 1.28 |
| No cryoprotector | 10% | 1.41 |
| | – | 2.95 |

ND: not determined

glucose, sucrose, dextran, and trehalose at different concentrations were investigated in this study. As shown in Table 4, after lyophilization with cryoprotective agents, mean particle sizes of all the samples were 1.06~15.81 times larger than in the original dispersions. With 2%, 5% or 10% dextran and 10% mannitol, the particle sizes were even larger than those of the lyophilized lipid nanoparticles without a cryoprotector. However, in the case of 10% trehalose, the mean particle size increased only slightly from 213 nm to 225 nm after lyophilization and encapsulation efficiency slightly decreased from 98% to 96% (as shown in Table 3), which made it the most effective cryoprotector among the candidates tested. Moreover, unlike other cryoprotectors, varying its concentration caused only insignificant alteration in particle size, in accordance with previous reports (Schwarz et al. 1994; Heiati et al. 1998). Therefore, 10% trehalose was chosen as the cryoprotector.

As shown in Table 3, all nanoparticles showed a reduced absolute value of zeta potential after lyophilization with trehalose and reconstitution, indicating decreased stability of the particles in some degree. Zeta potential was an important indication for the stability of the nanoparticle suspension. Larger absolute values of zeta potential usually indicated a higher charge density on the surface of the drug-loaded nanoparticles, which could cause strong repellent forces between particles, preventing aggregation in buffer solution and thus leading to better stability (Muhlen et al. 1998; Mehnert and Mader 2001).

When the freeze-dried SSLNs were redispersed, Span60-SSLN could not be completely redissolved while the resuspension of PEG-PE-SSLN appeared homogenous and complete. Freeze-drying and subsequent reconstitution of PEG-PE-SSLN did not result in any noticeable changes in particle size and size distribution (as shown in Table 3). For Span60-SSLN, the mean particle size increased from 275 nm to 327 nm after lyophilization and encapsulation efficiency decreased from 95% to 86%, which was a more obvious change than with PEG-PE-SSLN. Steric stabilization of SSLN by PEG may contribute to these results.

In conclusion, SSLNs provide a new approach to the delivery of PTX. The formulation possesses good drug loading

properties and exhibits excellent colloidal stability. Furthermore, PEG-coated SSLNs reduce the phagocytosis effect, which is expected to prolong circulation time in blood and potentially enhance tumor targeting efficiency. PEG-modified SSLNs for PTX exhibit the great advantage of avoiding the use of Cremophor EL® for the solubilization and formulation of PTX. Therefore, PEG-coated SSLNs may be a promising delivery carrier for PTX. Further studies are warranted to evaluate the potential therapeutic advantages of PEG-decorated SSLNs.

3. Experimental

PTX was purchased from Shanghai Hualian Pharmaceutical Co., Ltd. (Shanghai, China). Cremophor® EL was a gift from BASF Corporation (Ludwigshafen, Germany). Dynasan118 (Tristearin glyceride) was purchased from Shanghai No. 1 Chemical Plant (Shanghai, China). Soybean lecithin (L- α -phosphatidylcholine) of medicinal grade was purchased from Shanghai No. 1 Oils and Fats Factory (Shanghai, China). Miglyol812N (caprylic/capric triglycerides) was donated by Sasol Company (Johannesburg, South Africa). Sorbitan monostearate (Span 60), sucrose, sorbitol, mannitol, trehalose, and dextran were purchased from Sigma-Aldrich (St. Louis, MO, USA). Poly(ethylene glycol) – phosphatidylethanolamine (PEG-PE) was prepared in our laboratory with the molecular weight of PEG being 2000 Da. Sephadex G-75 was obtained from Pharmacia (Peapack, NJ, USA). Acetonitrile (Merck, Germany) was of HPLC grade and all other chemicals were of analytical grade. Hank's balanced salt solution, RPMI 1640 medium and fetal calf serum (FCS) were purchased from Gibco (Carlsbad, CA, USA).

3.1. Preparation of semi-solid lipid nanoparticles

Various formulations were prepared according to an orthogonal design (Table 1). The four factors were set as follows, A, Dynasan118; B, PTX; C, Miglyol812N; D, PEG-PE. SSLNs were prepared using the same method as our previous work (Wu et al. 2009). Briefly, 2 ml of lecithin solution in ethanol was blended with 5 ml of a mixture of PTX, Dynasan118 and Miglyol812N in acetone. The resulting mixture was added to 30 ml of emulsifier in water, followed by stirring at $70 \pm 2^\circ\text{C}$ for 4 h before acetone was removed. The suspension was then quickly dispersed in 60 ml of water at $0\sim 2^\circ\text{C}$ and solidified for 2 h. The SSLNs prepared with Span60 emulsifier (without PEG chain) or PEG-PE were designated as Span60-SSLN or PEG-SSLN, respectively, while blank-SSLN was prepared without adding PTX using PEG-PE as emulsifier. Each SSLN was prepared in triplicate.

3.2. TEM investigation, particle size and zeta-potential

TEM (JEM-1200EX, JEOL Company, Japan) was utilized to determine the morphology and size distribution of Span60-SSLN, PEG-PE-SSLN and blank-SSLN. Before observation, Span60-SSLN, PEG-PE-SSLN and blank-SSLN were stained with 2% (w/v) phosphotungstic acid and placed on copper grids to form films. Also, the particle size was confirmed with dynamic laser light scattering (Zetapals, Brookhaven, USA). The surface charge of the nanoparticles was determined by measuring the zeta potential. The zeta potential was measured by Zetapals (Zetapals, Brookhaven, USA). Samples for zeta potential measurement were diluted with water adjusted to a conductivity of $50\ \mu\text{S}/\text{cm}$ using sodium chloride. Measurements were performed in triplicate for all samples.

3.3. Encapsulation efficiency (EE)

PTX EE was analyzed by HPLC. Sephadex G-75 was pre-soaked with de-ionized water and packed into a $15\ \text{mm} \times 100\ \text{mm}$ column equilibrated with water. One aliquot of Span60-SSLN or PEG-PE-SSLN suspension of 400 microliters was applied to the column and eluted with water. The eluate was collected in 1 ml fractions in vials and subsequently analyzed by laser light scattering to identify the fraction(s) containing nanoparticles. Another aliquot of Span60-SSLN or PEG-PE-SSLN was directly dissolved in methanol and centrifuged at 12,000 rpm for 30 min. The amount of PTX in the suspension was analyzed by HPLC, representing the original amount of PTX in 400 μl of Span60-SSLN or PEG-PE-SSLN suspension. Each analysis was performed in triplicate. Drug EE was defined as the ratio of the actual amount of PTX loaded in the nanoparticles to the original amount of PTX in the Span60-SSLN or PEG-PE-SSLN suspension. The equation is as follows:

$$\text{Encapsulation efficiency (EE)} = \frac{\text{Actual amount of PTX loaded in nanoparticles}}{\text{Theoretical amount of PTX loaded in nanoparticles}} \times 100\%$$

3.4. Differential scanning calorimetry (DSC)

The physical state of PTX inside the nanoparticles was characterized by thermal analysis (DSC204/1/G Phoenix, Germany). The samples were sealed in aluminum pans and purged with dry nitrogen at a flow rate of 2 ml/min. The DSC scan was recorded from 10 to 300 °C at a heating rate of 10 °C/min, using an empty pan as reference.

3.5. *In vitro* drug release

The *in vitro* release of PTX from Span60-SSLN and PEG-PE-SSLN was investigated by membrane dialysis at 37 °C. A Spectra/Pro® regenerated cellulose dialysis membrane with a molecular weight cut-off size of 14,000 Da was used, and the nanoparticle suspension was dialyzed against pH 7.4 phosphate buffered saline (PBS) containing 0.1% (w/v) Tween 80. The release medium was shaken at 100 rpm. At fixed time intervals, 1 ml of the release medium was withdrawn and replaced with 1 ml of fresh medium. HPLC was used to determine the concentration of PTX and the cumulative percentage of PTX released was calculated accordingly.

3.6. Phagocytic uptake of semi-solid lipid nanoparticles

Care and handling of animals and protocols of animal experiments were approved by the Fudan University Animal Care and Use Committee in accordance with US NIH Guidelines. Murine peritoneal monocyte-macrophages (MPM) were employed to study the phagocytic uptake of Span60-SSLNs and PEG-PE-SSLNs. Mouse peritoneal exudates were obtained on the 4th day after intraperitoneal injection of 1 ml of 10 µg/ml dextran, and were washed twice with Hank's balanced salt solution followed by centrifugation at 3,000 rpm for 10 min at 4 °C and then resuspended in RPMI 1640 medium supplemented with 10% fetal bovine serum (FBS). Cells were seeded on a culture dish at a density of 1.0×10^5 cells per dish. After incubation at 37 °C for 3 h, non-adherent cells were removed by washing with RPMI 1640 to obtain a peritoneal macrophage monolayer (Aramaki et al. 1995). 500 µL of Span60-SSLN or PEG-PE-SSLN suspension was added to 1 ml of MPM in RPMI 1640 medium and incubated at 37 °C for 30 min. After further incubation in an ice bath in order to stop phagocytosis they were centrifuged at 3,000 rpm for 10 min. The supernatant was discarded, and the precipitate was resuspended in PBS, sonicated, and centrifuged at 12,000 rpm for 20 min. The supernatant was analyzed by HPLC. Opsonization of the SSLNs was evaluated by incubating 0.5 ml of Span60-SSLN or PEG-PE-SSLN with 1 ml of MPM in 5 ml of 2% fresh pooled mouse plasma at 37 °C for 30 min under shaking. Each sample was assayed in triplicate.

3.7. Lyophilization of semi-solid lipid nanoparticles

PEG-PE-SSLNs were lyophilized in the presence of 2%, 5% or 10% glucose respectively, and PEG-PE-SSLNs were also lyophilized in the presence of sucrose, sorbitol, mannitol, dextran or trehalose at the same three concentrations. Samples were frozen at -70 °C for 72 h and immediately placed in a freeze-drying chamber (LGJ0.5-II, Academy of Military Medicine Science Experiment Instruments, China). The same procedures were carried out in the absence of cryoprotective agents as a control. Span 60-SSLNs and blank-SSLNs were freeze-dried in the presence of 10% trehalose. Sample reconstitution was performed by adding 2 ml of water to the dried SSLNs followed by a mild manual shaking 5 min later.

3.8. HPLC analysis of paclitaxel

The HPLC system consisted of an LC 10ATvp pump (Shimadzu, Kyoto), a Rheodyne Model 7725 injection valve equipped with a 20 µl loop (Torrance, USA), an SPD-10A UV-VIS detector (Shimadzu, Kyoto), and an HS 2000 series chromatographic workstation (Hangzhou Yingpu Co., Hangzhou, China). The column used was a Hypersil C₁₈ 150 mm × 4.6 mm (10 µm, Yilite, Dalian, China). The UV detector was set at 227 nm. Isocratic elution was performed using acetonitrile/water (58:42, v/v) at a flow rate of 1.0 ml/min.

References

Allen TM (1994) The use of glycolipids and hydrophilic polymers in avoiding rapid uptake of liposomes by the mononuclear phagocyte system. *Adv Drug Del Rev* 13: 285–309.

Ana V, Howard G, Orla M, Maria JA (2004) Transport of PLA-PEG particles across the nasal mucosa: effect of particle size and PEG coating density. *J Control Release* 98: 231–244.

Aramaki Y, Akiyama K, Hara T, Tsuchiya SS (1995) Recognition of charged liposomes by rat peritoneal and splenic macrophages: effects

of fibronectin on the uptake of charged liposomes. *Eur J Pharm Sci* 3: 63–70.

Bocca C, Caputo O, Cavalli R, Gabriel L, Miglietta A, Gasco MR (1998) Phagocytic uptake of fluorescent stealth and non-stealth solid lipid nanoparticles. *Int J Pharm* 175: 185–193.

Chen DB, Yang TZ, Lv WL, Zhang Q (2002) *In vitro* and *in vivo* study of two kinds of long-circulating solid lipid nanoparticles containing paclitaxel. *Acta Pharm Sin* 37: 54–58.

Dubernet C (1995) Thermoanalysis of microspheres. *Thermochim Acta* 248: 259–269.

Evora C, Soriano I, Rogers RA, Shakesheff KM, Hanes J, Langer R (1998) Relating the phagocytosis of microparticles by alveolar macrophages to surface chemistry: the effect of 1,2-dipalmitoylphosphatidylcholine. *J Control Release* 51: 143–152.

Freitas C, Müller RH (1998) Spray-drying of solid lipid nanoparticles (SLNTM). *Eur J Pharm Biopharm* 46: 145–151.

Gabizon A, Catane R, Uziely B, Kaufman B, Safra T, Cohen R, Martin F, Huang A, Barenholz Y (1994) Prolonged circulation time and enhanced accumulation in malignant exudates of doxorubicin encapsulated in polyethylene-glycol coated liposomes. *Cancer Res* 54: 987–992.

Garcia-Fuentes M, Alonso MJ, Torres D (2005) Design and characterization of a new drug nanocarrier made from solid-liquid lipid mixtures. *J Colloid Interface Sci* 285: 590–598.

Gradishar WJ (2006) Albumin-bound paclitaxel: a next-generation taxane. *Expert Opin Pharmacother* 7: 1041–1053.

Gradishar WJ, Tjulandin S, Davidson N, Shaw H, Desai N, Bhar P, Hawkins M, O'Shaughnessy J (2005) Phase III trial of nanoparticle albumin-bound paclitaxel compared with polyethylated castor oil-based paclitaxel in women with breast Cancer. *J Clin Oncol* 23: 7794–7803.

Heiati H, Tawashi R, Phillips NC (1998) Drug retention and stability of solid lipid nanoparticles containing azidothymidine palmitate after autoclaving, storage and lyophilisation. *J Microencaps* 15: 173–184.

Jenning V, Thünnemann AF, Gohla SH (2000) Characterisation of a novel solid lipid nanoparticle carrier system based on binary mixtures of liquid and solid lipids. *Int J Pharm* 199: 167–177.

Klivanov AL, Maruyama K, Beckerley AM, Torchilin VP, Huang L (1991) Activity of amphipathic poly (ethylene glycol) 5 000 to prolong the circulation time of liposomes depends on the liposome size and is unfavorable for immunoliposomes binding to target. *Biochim Biophys Acta* 1062: 142–148.

Lamprecht A, Bouligand Y, Benoit JP (2002) New lipid nanocapsules exhibit sustained release properties for amiodarone. *J Control Release* 84: 59–68.

Lifang Wu, Cui Tang, Chunhua Yin (2009) Folate-mediated solid-liquid lipid nanoparticles for paclitaxel coated poly(ethylene glycol). *Drug Devel Ind Pharm*, doi 10.3109/03639040903244472.

Liggins RT, Hunter WL, Burt HM (1997) Solid-state characterization of paclitaxel. *J Pharm Sci* 12: 1458–1463.

Muhlen A, Schwarz C, Mehnert W (1998) Solid lipid nanoparticles (SLN) for controlled drug delivery-drug release mechanism. *Eur J Pharm Biopharm* 45: 149.

Mehnert W, Mader K (2001) Solid lipid nanoparticles: production, characterization and applications. *Advanced. Drug Del Rev* 47: 165–196.

Müller RH, Mäder K, Gohla S (2000) Solid lipid nanoparticles (SLN) for controlled drug delivery – a review of the state of the art. *Eur J Pharm Biopharm* 50: 161–177.

Prior S, Gander B, Blarer N, Merkle HP, Subira ML, Irache JM, Gamazo V (2002) *In vitro* phagocytosis and monocyte-macrophage activation with poly(lactide) and poly(lactide-co-glycolide) microspheres. *Eur J Pharm Sci* 15: 197–207.

Rudt S, Müller RH (1992) *In vitro* phagocytosis assay of nano- and microparticles by chemiluminescence. I: Effect of analytical parameters, particle size and particle concentration. *J Control Release* 22: 263–272.

Sahoo SK, Ma W, Labhasetwar V (2004) Efficacy of transferring conjugated paclitaxel-loaded nanoparticles in a murine model of prostate cancer. *Int J Cancer* 112: 335–340.

Schwarz C, Mehnert W, Müller RH (1994) Lyophilization of solid lipid nanoparticles (SLN). *Eur J Pharm Sci* 2: 177.

Schwarz C, Mehnert W (1997) Free-drying of drug-free and drug-loaded solid lipid nanoparticles (SLN). *Int J Pharm* 157: 171–179.

Song D, Hsu LF, Au JLS (1996) Binding of paclitaxel to plastic glass container and protein under *in vitro* conditions. *J Pharm Sci* 85: 29–31.

Spencer CM, Faulds D (1994) Paclitaxel. *Drugs* 48: 794–847.

Szebeni J, Muggia FM, Alving CR (1998) Complement activation by Cremophor EL as a possible contributor to hypersensitivity to paclitaxel: an *in vitro* study. *J National Cancer Institute* 90: 300–306.

ORIGINAL ARTICLES

- Westesen K, Bunjes H, Koch MHJ (1997) Physicochemical characterization of lipid nanoparticles and evaluation of their drug loading capacity and sustained release potential. *J Control Release* 48: 223–236.
- Woodle MC, Lasic DD (1992) Sterically stabilized liposomes. *Biochim Biophys Acta* 1113: 171–199.
- Zara GP, Cavalli R, Bargoni A, Fundarò A, Vighetto D, Gasco MR (2002) Intravenous administration to rabbits of non-stealth and stealth doxorubicin-loaded Solid Lipid Nanoparticles at increasing concentrations of stealth agent: pharmacokinetics and distribution of doxorubicin in brain and other tissues. *J Drug Target* 10: 327–335.
- Zhang ZP, Feng SS (2006) The drug encapsulation efficiency, *in vitro* drug release, cellular uptake and cytotoxicity of paclitaxel-loaded poly (lactide)–tocopheryl polyethylene glycol succinate nanoparticles. *Biomaterials* 27: 4025–4033.